THE JOURNAL OF BIOLOGICAL CHEMISTRY
Vol. 275, No. 28, Issue of July 14, pp. 21130–21139, 2000

Printed in U.S.A.

Antioxidant/Pro-oxidant Equilibrium Regulates HIF-1α and NF-κB Redox Sensitivity

EVIDENCE FOR INHIBITION BY GLUTATHIONE OXIDATION IN ALVEOLAR EPITHELIAL CELLS*

Received for publication, January 28, 2000, and in revised form, April 11, 2000
Published, JBC Papers in Press, May 4, 2000, DOI 10.1074/jbc.M000737200

John J. E. Haddad‡, Richard E. Olver§, and Stephen C. Land¶

From the Oxygen Signaling and §Lung Membrane Transport Groups, Center for Research into Human Development, Tayside Institute of Child Health, Faculty of Medicine, Ninewells Hospital and Medical School, University of Dundee, Dundee, DD1 9SY, Scotland, United Kingdom

The O_2 and redox-sensitive transcription factors hypoxia inducible factor-1α (HIF-1α) and nuclear factor-κB (NF-κB) are differentially regulated in the alveolar epithelium over fetal to neonatal oxygen tensions. We have used fetal alveolar type II epithelial cells to monitor their regulation in association with redox responsiveness to antioxidant pretreatment *in vitro*. *N*-Acetyl-L-cysteine, a glutathione (GSH) precursor and a potent scavenger of reactive oxygen species, induced HIF-1α and ameliorated NF-κB nuclear abundance and DNA binding activity, respectively, in a dose-dependent manner. Analysis of variations in glutathione homeostasis at ascending ΔpO_2 regimen with *N*-acetyl-$_L$-cysteine reveals increased GSH at the expense of the oxidized form of glutathione (GSSG), thereby shifting GSH/GSSG into reduction equilibrium. Pyrrolidine dithiocarbamate (PDTC), which exerts both antioxidant and pro-oxidant effects, provoked a substantial increase in HIF-1α nuclear abundance, with no apparent effect on its activation. PDTC reduced NF-κB nuclear abundance and its inhibitory effects on binding activity are dose-dependent. Assessment of glutathione homeostasis with PDTC shows increasing levels of GSSG at the expense of GSH, lowering GSH/GSSG in favor of an oxidative equilibrium. Our results indicate the hypoxic activation of HIF-1α and the hyperoxic induction of NF-κB in the fetal epithelium is redox-sensitive and, thus, tightly regulated by the GSH/GSSG equilibrium. This highlights glutathione as a key regulatory component for determining genetic responsiveness to oxidant/antioxidant imbalance in normal lung development and pathophysiological conditions.

In normal health, enzymatic and nonenzymatic antioxidants serve to balance the intracellular production of reactive oxygen species (ROS),[1] thereby delaying or inhibiting the destructive oxidation of molecular components within the cellular milieu (1, 2). The potential for oxidative damage is greatly augmented however, if the antioxidant buffering capacity of the organ system is insufficiently expressed to contain pro-oxidant events. This is particularly critical in the lung at birth where the transition from placental to pulmonary respiration necessitates a rapid shift in oxygenation of the alveolar epithelial gas exchange surfaces from fetal (23 torr) to neonatal pO_2 (70–100 torr). As the enzymatic and nonenzymatic antioxidant capacities of the fetal lung are 3–6-fold lower compared with those of late neonates and adult (7 and references therein, 25), the potential for pro-oxidant events within the distal lung epithelium is substantially heightened at birth.

The restitution of redox balance following oxidative stress depends upon the adaptive coordination of responses among redox-associated signaling pathways, genetic regulatory factors, and antioxidants (3, 4). The tripeptide thiol L-γ-glutamyl-L-cysteinyl-glycine, or GSH, is a ubiquitous cellular nonessential sulfhydryl amino acid, which plays an important role in maintaining intracellular redox balance and in augmenting cellular defenses in oxidative stress (5–7). Glutathione participation in the physiology of cellular metabolism reflects the importance of this molecule in (i) detoxification of highly reactive peroxides by conjugation of electrophiles and metals through the glutathione peroxidase-coupled reaction (8); (ii) maintenance of intracellular protein integrity by reducing disulfide linkages and regulating their synthesis (5); (iii) regulation of cellular redox equilibrium (9); (iv) governing signaling pathways in neuro-immune-endocrine interactions by acting as a neurotransmitter and an immunopharmacological reducing thiol (10); (v) facilitating membrane trafficking of reactive chemicals and, in some cases, augmenting the formation of essential biological mediators (11); and (vi) regulation of the expression and activation of redox-sensitive transcription factors to stress-evoked responses (3, 12, 40). Recently, Griffith and Mulcahy (5) and Rusakow *et al.* (9) demonstrated that the glutathione biosynthetic pathway forms an important determinant of the effectiveness of an antioxidant approach in chemotherapy and pulmonary oxygen toxicity, thereby highlighting the pharmacological potential of this thiol in the treatment of redox-linked disease states.

Pharmacological manipulation of GSH by pro- and antioxidants directly modulates the activity of transcription factors in response to various stimuli, including changes in the availability of oxygen (3, 13, 14). Among those which bear particular significance to oxygen-linked redox stresses are hypoxia induc-

* This work was supported by grants from the Medical Research Council, Anonymous Trust, and Tenovus-Scotland (to S. C. L.). The costs of publication of this article were defrayed in part by the payment of page charges. This article must therefore be hereby marked "*advertisement*" in accordance with 18 U.S.C. Section 1734 solely to indicate this fact.

‡ This work is part of the doctoral dissertation of this author, who is a recipient of the George John Livanos Prize Ph.D. scholarship (London).

¶ To whom reprint requests and correspondence should be addressed. Tel.: 44 (0) 1382 496268; Fax: 44 (0) 1382 632597; E-mail: s.c.land@dundee.ac.uk.

[1] The abbreviations used are: ROS, reactive oxygen species; GSH, glutathione; HIF-1α, hypoxia inducible factor-1α; NF-κB, nuclear factor-κB; NAC, *N*-acetyl-L-cysteine; PDTC, pyrrolidine dithiocarbamate; GSSG, the oxidized form of glutathione; fATII, fetal alveolar type II; γ-GCS, γ-glutamylcysteine synthetase; IκB, inhibitor κB.

ible factor-1α (HIF-1α) and nuclear factor-κB (NF-κB), each differentially potentiated by oxidative conditions (7, 15, 16). HIF-1α, first identified as a rate-limiting regulatory component in the hypoxic induction of erythropoietin, is selectively stabilized in hypoxia whereupon it is translocated to the nucleus and activates the expression of genes promoting vascular development, glycolytic metabolism, and also cell cycle events (16, 17). The activation of HIF-1α is therefore consistent with the significant role that this factor plays in coordinating adaptive responses to hypoxia (16–18). NF-κB (*Rel*) is a DNA binding factor that is maintained in the cytosol as a heterodimer in complex with its inhibitory subunit, IκB. Upon activation by inflammatory signals (such as cytokines) or pro-oxidant stresses, IκB dissociates allowing the *Rel* dimers of this factor to translocate to the nucleus and activate genes particularly involved in modulating the response of the cell to oxidative injury (19).

We have previously shown that both HIF-1α and NF-κB are differentially active over ranges of oxygen tension, which recreate the elevation in pO_2 within the perinatal lung that is coincident with the onset of ventilation (7). To determine how altered redox status within the alveolar epithelium may dictate genetic control between HIF-1α and NF-κB over relevant shifts in pO_2, we evaluated the effect of the antioxidants *N*-acetyl-L-cysteine (NAC) and pyrrolidine dithiocarbamate (PDTC) in modulating the genetic response of the alveolar epithelium to oxidative stress. Since the discovery of biologically occurring free radicals, NAC has been used as a probe in detecting the biochemical basis of oxidative-induced lung injury both *in vitro* and *in vivo* experimental and clinical models (20). NAC has the capacity to negatively buffer electrophiles and is thus an antioxidant with cytoprotective potential. In addition to its direct antioxidant effects, NAC may also serve as a precursor for cysteine and glutathione biosynthesis, thereby positively buffering the cellular pool of nucleophilic species (21). PDTC is a member of the dithiocarbamate family, known to exert both antioxidant and pro-oxidant effects in cells (22). Reduced dithiocarbamate is readily oxidized by reactive oxygen and nitrogen species to generate dithiocarbamate thiol radicals and thiuram disulphides. As potent electrophiles, these readily induce the oxidation of GSH leading to the formation of GSSG, the oxidized form of glutathione (23). Pretreatment with NAC or PDTC has been shown to suppress the activation of NF-κB and enhance that of activator protein 1 (3). Furthermore, although PDTC-induced inhibition of NF-κB has often been attributed to its antioxidant, radical-scavenging properties, recent evidence suggests that this inhibitory effect could be mediated by direct oxidation of the thiol containing cysteinyl group critical to the activity of this transcription factor (24).

The present study was undertaken to investigate the role that these modulators of glutathione biosynthesis play to in determining the response of the perinatal alveolar epithelium at the gene level over fetal to neonatal oxygen shifts and to probe whether their effects are mediated by altering redox potential via the GSH/GSSG equilibrium.

EXPERIMENTAL PROCEDURES

All experimental procedures involving the use of live animals were reviewed and approved under the Animals (Scientific Procedures) Act, 1986 (United Kingdom).

Chemicals—Unless otherwise indicated, all chemicals of the highest analytical grade were purchased from Sigma.

Primary Cell Cultures—Fetal alveolar type II (fATII) epithelial cells were isolated from lungs of fetuses taken from the uteri of pregnant rats at day 19–20 of gestation, essentially as described elsewhere (7). The change in oxygen equilibrium from fetal (~3%) to postnatal environments constitutes a potential signaling mechanism within the perinatal lung (25). Consequently, shifts in pO_2 relevant to the fetal lung in preterm and post-term neonatal periods were recreated using variable O_2 incubators. fATII cells, with or without NAC or PDTC pretreatments, were cultured for 24 h at fetal alveolar pO_2 (23 torr, ≈3% O_2, 5% CO_2) followed by a control period at the same pO_2 or re-equilibrated to early postnatal alveolar pO_2 (76 torr, ≈10% O_2, 5% CO_2), mild hyperoxia (normoxia) (152 torr, ≈21% O_2, 5% CO_2), and severe hyperoxia (722 torr, ≈95% O_2, 5% CO_2) for 4 h at 37 °C. In each case, and under conditions of independent pretreatments, the adenylate energy charge remained ≥0.7, and transepithelial monolayer resistance was monitored as ≥250 Ω cm^2.

Cell Harvesting, Nuclear Protein Extraction, and Western Analysis—Nuclear extracts were prepared from monolayer filters of fATII cells grown under hypoxia or hyperoxia, essentially as detailed elsewhere (7, 26), with minor modifications. Nuclear proteins (20–25 μg) were resolved by 7.5% SDS-polyacrylamide gel electrophoresis, blotted onto nitrocellulose membranes, transferred into Tris-buffered saline, and the nonspecific binding sites were blocked for 1 h at room temperature. Monoclonal IgG anti-HIF-1α (Novus Biologicals Co.) and polyclonal IgG p65 anti-NF-κB (Santa Cruz Biotechnology, Santa Cruz, CA) antibodies were used for primary detection. Anti-rabbit Ig-biotinylated antibody (Amersham Pharmacia Biotech) was employed for secondary detection followed by the addition of streptavidin-horseradish peroxidase conjugate. The membrane was enhanced (ECL; Amersham Pharmacia Biotech) and exposed to an automatic x-ray film processor. β-Actin standard was used as a reference for semiquantitative loading in parallel lanes for each variable. Blots were digitized using a transilluminating scanner, and the density of bands relative to β-actin were determined using UN-Scan-IT 32-bit automated digitizing system (version 5.1, Silk Scientific Corp., Orem, UT). Data from at least four independent blots were pooled, averaged, and plotted as a percentage of maximal abundance/activation relative to control at static pO_2.

Electrophoretic Mobility Shift Assay and DNA Binding Activity—Custom deoxyoligonucleotide probe sequences were purchased from Genosys: HIF-1α, 5′-GCCCTACGTGCTGTCTCA-3′; and NF-κB, 5′-AGTTGAGGGGACTTTCCCAGGC-3′ (binding sequences are underlined). Gel-purified double-stranded DNA was end-labeled with [γ-^{32}P]ATP (NEN Life Science Products). Identical amounts of radioactive probe (1–2 × 10^4 counts·min^{-1}) were added to binding reactions containing 1–5 μg of fATII nuclear extracts in a final volume of 40 μl in DNA binding buffer (7). Reaction mixtures were incubated for 30 min at 25 °C before separating on nondenaturing 4% polyacrylamide gels at room temperature and subjected to electrophoresis with 1:10 5× Tris-Borate-EDTA buffer. A nonspecific competitive polydeoxyinosinic-deoxycytidylic acid (poly(dI-dC)) (Amersham Pharmacia Biotech) was added to reaction mixtures after the addition of labeled probe. Gels were transferred to ion-exchange chromatography paper, vacuum dried, and quantitated by phosphorimaging using a Canberra-Packard Instant Imager.

NAC and PDTC Pretreatments—Stock solutions of NAC (1125 mM) and PDTC (1125 μM) were prepared in deionized water and stored at 4 °C for up to 2 weeks. fATII cells grown to confluence were pretreated for 24 h at 37 °C with NAC (0 (control), 1, 10, and 50 mM) or PDTC (0, 10, 50 and 100 μM) before exposure to various fetal to neonatal oxygen tensions for 4 h. After each treatment, fATII cells were washed with pre-equilibrated Hanks' balanced salt solution and centrifuged, and nuclear extracts were prepared, as described above.

Glutathione Determination and Assessment of Redox Equilibrium—Reduced (GSH) and oxidized (GSSG) glutathione concentrations were determined enzymatically with methylglyoxal by the method originally reported by Bergmeyer (27), with significant modifications (7). fATII epithelial cells grown on monolayers, with or without NAC or PDTC pretreatments, were washed twice with ice-cold phosphate-buffered saline, and immediately 500 μl of 7% perchloric acid was added to the medium and cells were scraped. The slurry was then centrifuged to precipitate the protein formed and the supernatant snap frozen on liquid nitrogen. Samples were neutralized with a known volume of 3 M $KHCO_3$, and GSH/methylglyoxal-linked changes in absorbance at 240 (GSH) and 340 nm (GSSG) were recorded spectrophotometrically (7). Protein content was reconstituted in 1 M NaOH and determined by Bradford (28). Results are expressed as μmol·mg^{-1} protein.

In Vitro Treatment of Nuclear Extracts with Exogenous Glutathione—In vitro experiments with glutathione were performed by incubating 5 μg of nuclear extracts of fATII cells exposed to various ΔpO_2 regimen with different concentrations of GSH and GSSG for 15 min on ice. The total glutathione (GSH + GSSG) concentration/reaction mixture (40 μl) was adjusted to 100 nmol/ml, and the ratio ([GSH] + [GSSG])/([GSSG]) was modulated such that [GSSG] was increased at the expense of [GSH]. Ratios were adjusted to final values of 100, 50, 10, 5, 2, 1.25, and 1. After incubation period samples were assayed for the

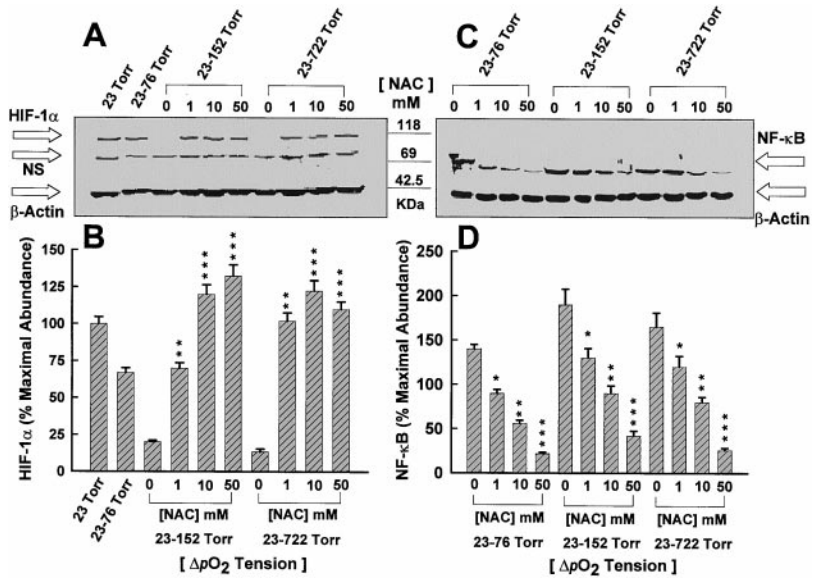

FIG. 1. **Effects of NAC pretreatments on nuclear abundance of HIF-1α and NF-κB under various oxygen tensions.** *A,* dose-dependent variations in HIF-1α nuclear abundance as assessed with immunoblotting showing protein abundance with different concentrations of NAC. β-Actin is shown as an internal reference for semiquantitative loading in each lane. *NS*, nonspecific. *B,* the percentage relative maximal abundance of HIF-1α against that obtained under activating conditions (23 and 23→76 torr ΔpO_2) without NAC pretreatment (**, $p < 0.01$; ***, $p < 0.001$, as compared with control (0 mM NAC)). *C,* dose-dependent variations in NF-κB nuclear abundance as assessed with Rel-A anti-p65 showing protein abundance with different concentrations of NAC. *D,* the percentage relative maximal abundance of NF-κB against the control values obtained without NAC pretreatment (*, $p < 0.05$; **, $p < 0.01$; ***, $p < 0.001$, as compared with control). The histograms represent the mean values and the error bars the S.E. of the relative intensity of the bands of four independent experimental preparations.

binding activities of HIF-1α and NF-κB as indicated above. All nuclear extracts tested prior to the addition of glutathione had undetectable levels of GSH or GSSG (≪0.01 nmol/ml).

Assessment of the Adenylate Charge Ratio, Trypan Blue Exclusion, and Tetrazolium Reduction as Independent Indices of Cell Viability Following Pretreatment with Either NAC or PDTC—Evaluation of the adenylate high energy phosphate content as an index of cell viability and metabolic activity was based on the energy charge ratio determination for various treatments according to Atkinson (29). Trypan blue (0.4%) exclusion indicates the relative percentage of cells that are viable with respect to various treatments, such that the viability was greater than 90% with either NAC or PDTC pretreatments. Tetrazolium salt 3-(4,5-dimethylthiazol-2-yl)-2,5-diphenyl tetrazolium bromide cleavage into formazan blue by the mitochondrial enzyme succinate dehydrogenase is considered a reliable assessment of the degree of cell survival (30).

Data Handling and Statistical Analysis—Experimental results are expressed as mean ± S.E. Statistical analysis was performed by one way analysis of variance (ANOVA), followed by *post hoc* Tukey's test to determine mean separation significance among treatments. The *a priori* acceptable level of significance at 95% confidence was considered $p < 0.05$.

RESULTS

NAC Attenuation of HIF-1α and NF-κB Nuclear Abundance—Variation in nuclear protein abundance of HIF-1α and NF-κB at various ΔpO_2 shifts was investigated by Western analysis. Within the limits of the oxygen tensions investigated in our experiments, HIF-1α nuclear abundance was maximally elevated in cultures that were maintained constantly at 23 torr. On mild oxygenation to 76 torr (the estimated pO_2 of the distal lung within the first series of breaths at birth), the relative level of HIF-1α nuclear abundance was significantly diminished but remained well above that of cultures exposed to moderate and severe hyperoxic shifts where nuclear protein levels were barely detectable (Fig. 1*A*). A 24-hour preincubation with NAC in cultures maintained at 23 torr preserved the nuclear abundance of HIF-1α in a dose-dependent manner independently of the relative level of hyperoxic shift (Fig. 1*A*). Fig. 1*B* presents the densitometric analysis of HIF-1α abundance referenced to β-actin (**, $p < 0.01$ and ***, $p < 0.001$, as compared with cultures without pretreatment (0 mM NAC)). These events were accompanied by a dose-dependent increase in the GSH/GSSG (Table I, discussed below). In contrast to the O_2 and NAC activity pattern of HIF-1α, the hyperoxic induction of NF-κB nuclear translocation was substantially inhibited by NAC, again, in a dose-dependent manner (Fig. 1*C*). The maximum inhibition is evident with 50 mM NAC at all oxygen tensions studied, whereas the lowest concentration tested (1 mM) showed mild, though significant, attenuation of the p65 subunit (Fig. 1, *C* and *D*). Densitometric analysis of NF-κB nuclear abundance in reference to β-actin is given in Fig. 1*D* (*, $p < 0.05$; **, $p < 0.01$; ***, $p < 0.001$, as compared with cultures without pretreatment).

PDTC Attenuation of HIF-1α and NF-κB Nuclear Abundance—PDTC pretreatment of cultures exposed to each ΔpO_2 regimen produced a similar pattern of HIF-1α and NF-κB nuclear accumulation as noted for NAC treatments. The attenuation of HIF-1α nuclear accumulation with increasing pO_2 is blocked in a dose-dependent manner by increasing PDTC (Fig. 2, *A* and *B*, the latter presenting densitometric analysis of HIF-1α abundance referenced to β-actin (*, $p < 0.05$; **, $p < 0.01$; ***, $p < 0.001$; as compared with cultures without pretreatment (0 μM PDTC)). Fig. 2*C* shows the dose-dependent inhibitory effect of PDTC on NF-κB nuclear abundance under various ΔpO_2. The maximum inhibition is evident with 100 μM PDTC at all oxygen tensions studied, whereas the lowest concentration tested (10 μM) showed mild, though significant, attenuation of the p65 subunit (Fig. 2, *C* and *D*). Densitometric analysis of NF-κB nuclear abundance in reference to β-actin is given in Fig. 2*D* (*, $p < 0.05$; **, $p < 0.01$; ***, $p < 0.001$; as compared with cultures without pretreatment (0 μM PDTC)). Note that the effective concentration of PDTC under each ΔpO_2 regimen lies within the 10^{-4}-10^{-6} M range, whereas that of NAC lies in the range of 10^{-2}-10^{-3} M. The PDTC-dependent changes in transcription factor activities were accompanied by a dose-dependent decrease in the glutathione ratio, as depicted in Table II (discussed below).

Electrophoretic Mobility Shift Assay Analysis of HIF-1α and NF-κB Activation Kinetics with NAC Pretreatment—The effect of NAC (0, 1, 10, and 50 mM) on DNA binding activity is shown for HIF-1α and NF-κB in Fig. 3, *A* and *C*, respectively. Exponential increase (HIF-1α) or decrease (NF-κB) of the binding activities are evident with increasing concentrations of NAC. Fig. 3, *B* (HIF-1α) and *D* (NF-κB), show histogram analysis of the dose-response curve (*, $p < 0.05$; **, $p < 0.01$; ***, $p < 0.001$; as compared with untreated cultures (0, Control)). The stimulatory (HIF-1α) and inhibitory (NF-κB) equilibrium constants (K_s and K_i) for NAC-dependent DNA binding activity were determined from the positive/negative linear regressions

TABLE I

Redox equilibrium assessment of glutathione ratio homeostasis under various oxygen ΔpO_2 regimen reported in fATII cells pretreated with NAC for 24 h at 37 °C

Data are mean ± S.E. NAC (0; $n = 7$), (1 mM; $n = 5$), (10 mM; $n = 5$), and (50 mM; $n = 5$). *, $p < 0.05$, **, $p < 0.01$; ***, $p < 0.001$, as compared to control (0), without NAC pretreatment. *n* refers to number of measurements taken from at least three independent cell filters, where the entire results were pooled and averaged.

ΔpO_2	Glutathione ratio ([GSH] + [GSSG])/([GSSG])			
	Degree of reduction equilibrium with NAC			
	mM			
Torr	0	1	10	50
152	2.51 ± 0.15	3.76 ± 0.17	5.97 ± 0.65*	7.55 ± 0.78**
23	3.78 ± 0.21	6.74 ± 0.28*	9.92 ± 0.76**	12.98 ± 0.97***
23 → 76	6.07 ± 0.36	7.57 ± 0.52	17.48 ± 1.38***	15.42 ± 1.14**
23 → 152	13.42 ± 0.84	7.16 ± 1.26	15.45 ± 0.75*	10.48 ± 0.92
23 → 722	3.60 ± 0.18	4.53 ± 0.43	6.91 ± 0.54*	9.23 ± 0.88**

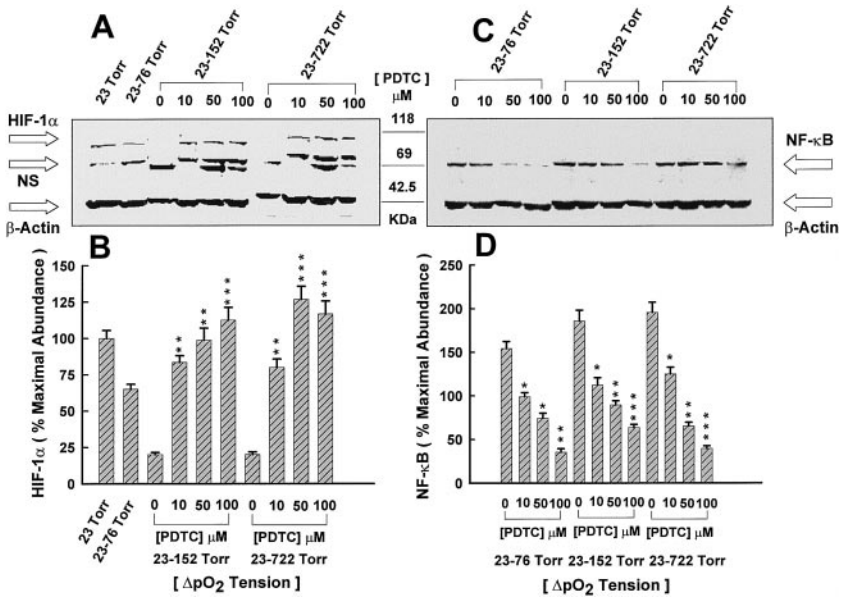

FIG. 2. **Effects of PDTC pretreatments on nuclear abundance of HIF-1α and NF-κB under various oxygen tensions.** *A,* dose-dependent variations in HIF-1α nuclear abundance as assessed with immunoblotting, showing protein abundance with different concentrations of PDTC. β-Actin is shown as an internal reference for semiquantitative loading in each lane; *NS*, nonspecific. *B,* the percentage relative maximal abundance of HIF-1α against that obtained at 23 and 23→76 torr ΔpO_2 without PDTC pretreatment (**, $p < 0.01$; ***, $p < 0.001$, as compared with control (0 μM PDTC)). *C,* dose-dependent variations in NF-κB nuclear abundance as assessed with RelA anti-p65, showing protein abundance with different concentrations of PDTC. *D,* the percentage relative maximal abundance of NF-κB against the control values obtained without PDTC pretreatment (*, $p < 0.05$; **, $p < 0.01$; ***, $p < 0.001$, as compared with control). The histograms represent the mean values and the error bars the S.E. of the relative intensity of the bands of five independent experimental preparations.

TABLE II

Redox equilibrium assessment of glutathione ratio homeostasis under various oxygen ΔpO_2 regimen reported in fATII cells pretreated with PDTC for 24 h at 37 °C

Data are mean ± S.E. PDTC (0; $n = 7$), (10 μM; $n = 5$), (50 μM; $n = 5$), and (100 μM; $n = 5$). *, $p < 0.05$; **, $p < 0.01$; ***, $p < 0.001$, as compared to control (0), without PDTC pretreatment. *n* refers to number of measurements taken from at least three independent cell filters, where the entire results were pooled and averaged.

ΔpO_2	Glutathione ratio ([GSH] + [GSSG])/([GSSG])			
	Degree of oxidation equilibrium with PDTC			
	μM			
Torr	0	10	50	100
152	2.56 ± 0.18	2.69 ± 0.17	2.16 ± 0.14	1.85 ± 0.10*
23	3.65 ± 0.20	3.01 ± 0.19	2.53 ± 0.16*	2.52 ± 0.14*
23 → 76	7.25 ± 0.32	4.42 ± 0.12*	3.09 ± 0.25**	2.63 ± 0.21***
23 → 152	10.87 ± 0.65	4.38 ± 0.15**	3.55 ± 0.22***	2.77 ± 0.18***
23 → 722	3.52 ± 0.12	3.05 ± 0.23	2.40 ± 0.13*	1.95 ± 0.11**

of the % stimulation/inhibition *versus* the concentration of NAC (mM) (Table III).

The specificity of the complexed bands, as detailed previously (7), was determined by incubating samples with mutant oligonucleotides (M-18 (HIF-1α); M-22 (NF-κB); 3-base pairs mutation), the addition of cold nonlabeled oligonucleotide competitor immediately before the probe, at 100-fold molar excess, and super shift analysis with specific antibodies for HIF-1α and NF-κB (RelA/p65) at 2 μg/reaction (Fig. 4, *A* and *B*).

Electrophoretic Mobility Shift Assay Analysis of HIF-1α and NF-κB Activation Kinetics with PDTC Pretreatment—The effect of PDTC (0, 10, 50, and 100 μM) on DNA binding activity is shown for HIF-1α and NF-κB in Fig. 5, *A* and *C*, respectively. No change (HIF-1α) and a significant decrease (NF-κB) of the binding activities are evident with increasing concentrations of PDTC. Fig. 5, *B* (HIF-1α) and *D* (NF-κB), shows a histogram analysis of the dose-response curve (**, $p < 0.01$; ***, $p < 0.001$; as compared with untreated cultures (0, Control)). The stimulatory (HIF-1α) and inhibitory (NF-κB) equilibrium constants (K_s and K_i) for PDTC-dependent DNA binding activity were determined from the positive/negative linear regressions of the % stimulation/inhibition *versus* the concentration of PDTC (μM) (Table III).

Variation in the Levels of GSH and GSSG with NAC Pretreatment—To assess whether NAC acts as a positive buffer of the glutathione pool, concentrations of GSH and GSSG were determined in extracts from cultures that had been pretreated with 10–50 mM NAC. The effect was to elevate cellular concen-

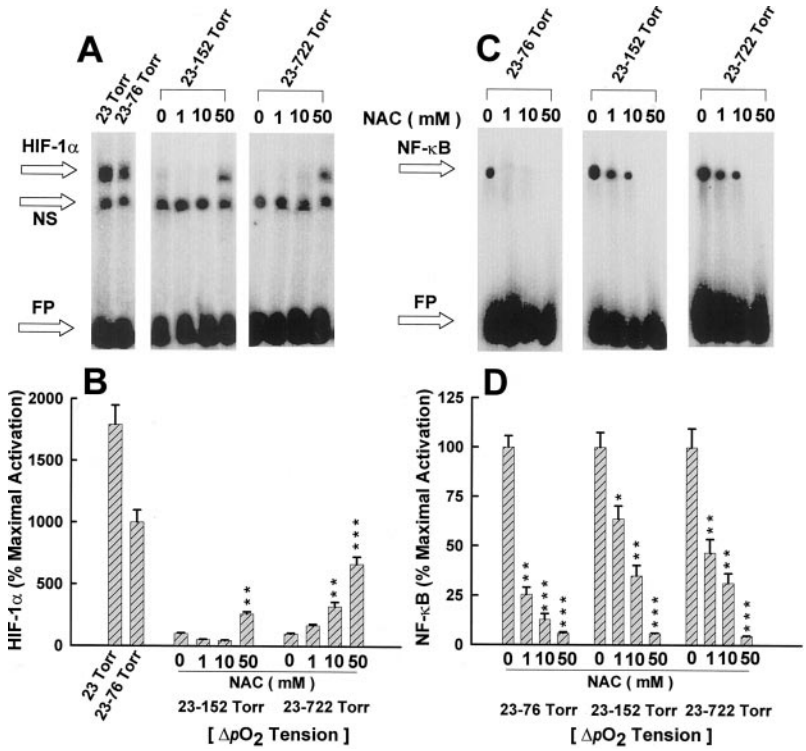

FIG. 3. **DNA consensus binding analysis for HIF-1α and NF-κB nuclear extracts (1–5 μg) with NAC.** *A,* HIF-1α activation state at 23 and 23→76 torr ΔpO_2 shifts (*FP*, free probe; *NS*, nonspecific). The stimulatory effects of NAC are evident over 23→152 and 23→722 torr, with apparent maximum activation at 50 mM. *B,* percentage analysis of the gross cpm relative to the intensity of the band of the control (0) at each pO_2 (**, $p < 0.01$; ***, $p < 0.001$). *C,* NF-κB activation status over ΔpO_2 shifts, where the inhibitory effects are prominent with increasing concentrations of NAC. *D,* percentage analysis of the gross cpm relative to the intensity of the band obtained without pretreatment (*, $p < 0.05$; **, $p < 0.01$; ***, $p < 0.001$). The histograms represent the mean values, and the error bars represent the S.E. of the relative intensity of the bands of four independent experiments.

TABLE III

Equilibrium constants extrapolated from the linear regression analysis obtained for the DNA-binding activity of HIF-1α and NF-κB in fATII epithelia pretreated with NAC or PDTC and exposed to ascending ΔpO_2 regimen

Data are the mean and error bars the S.E. of four independent experiments. K_s, NAC/PDTC stimulatory equilibrium constant (the effective concentration that induces 50% activation above control levels); K_i, NAC/PDTC inhibitory equilibrium constant (the effective concentration that inhibits activation by 50% below control levels); ND, nondetectable.

ΔpO_2	Stimulatory (K_s) and inhibitory (K_i) equilibrium constants			
	HIF-1α		NF-κB	
	mM	*μM*	*mM*	*μM*
Torr	NAC K_s	PDTC K_s	NAC K_i	PDTC K_i
23 → 76			1.95 ± 0.08	34.36 ± 3.92
23 → 152	24.44 ± 1.25	ND	16.04 ± 2.25	30.38 ± 3.35
23 → 722	0.41 ± 0.02	ND	11.97 ± 1.86	31.52 ± 2.87

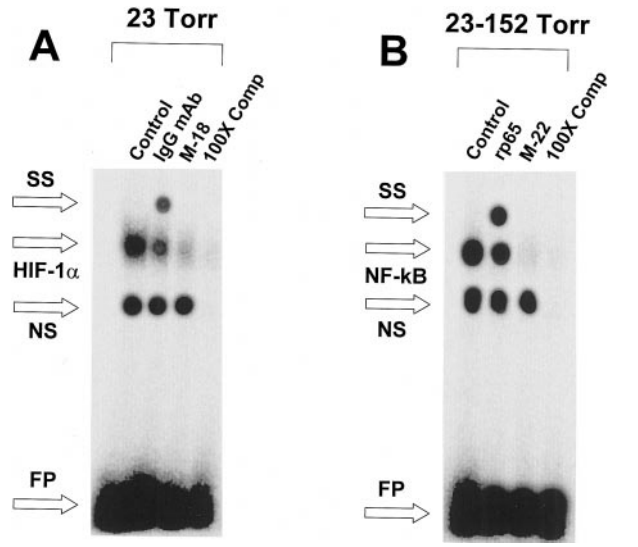

FIG. 4. **Specificity determination of the complexed bands obtained for HIF-1α and NF-κB.** *A,* HIF-1α binding complexes shown at 23 torr, with *arrows* indicating positions of the respective specific antibody-complexed supershifts (*FP*, free probe; *NS*, nonspecific; *SS*, supershift). The addition of the mutant oligonucleotide (M-18) and 100X-fold competitor completely abolished the binding of HIF-1α. *B,* NF-κB binding analysis with the corresponding displaced bands with anti-p65 shown at 23→152 torr ΔpO_2. The addition of the mutant oligonucleotide (M-22) and 100X-fold competitor completely abolished the binding of NF-κB. The data are representative of three separate experiments.

trations of GSH at the expense of GSSG, indicating that irrespective of the oxygen regime imposed, NAC potentiated a reduced cellular environment (Fig. 6). The corresponding ratios at different ΔpO_2 are given in Table I, with the maximum increase in GSH levels and glutathione redox ratio, coincident with the highest concentration of NAC used in this study (50 mM) at all oxygen tensions (**, $p < 0.01$; ***, $p < 0.001$; as compared with control (0 mM NAC)). NAC (1 mM) had no stimulatory effect on GSH elevation, and a 10 mM concentration increased the level of GSH at only 152 (Fig. 6*A*), 23→76 (Fig. 6*C*), and 23→722 (Fig. 6*E*) torr (*, $p < 0.05$; **, $p < 0.01$; ***, $p < 0.001$; as compared with control).

Variations in the Levels of GSH and GSSG with PDTC Pretreatment—To assess whether PDTC modulates GSSG/GSH, we determined the glutathione levels in extracts from cultures pretreated with PDTC at various ΔpO_2. PDTC elevated the concentration of GSSG at the expense of GSH, as evident from the decreasing ratio of total glutathione (GSH + GSSG) to that of GSSG, indicating oxidation of GSH. The corresponding ratios at different ΔpO_2 are given in Table II. The maximum increase in [GSSG] is evident with the highest concentration of PDTC used in this study (100 μM) at all oxygen tensions investigated (Fig. 7), except at 23 torr ($^{+}$, $p < 0.01$; $^{+++}$, $p < 0.001$; as compared with control (0 μM PDTC)). Likewise, 100 μM PDTC caused maximum decrease in GSH levels at all oxygen tensions, except at pO_2 = 152 torr (Fig. 7*A*) (*, $p < 0.05$; ***, $p < 0.001$; as compared with control). A PDTC concentration of 10 μM stimulated GSSG elevation at 23→152 torr (Fig. 7*D*), which decreased [GSH] at 23→76 and 23→152 torr (Fig. 7, *C* and *D*; *, $p < 0.05$; ***, $p < 0.001$; as compared with

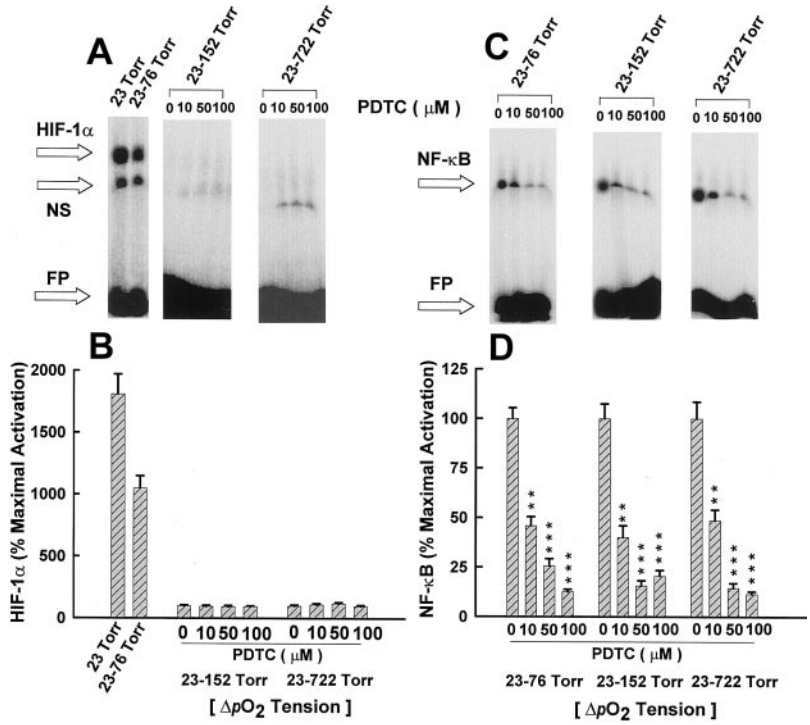

FIG. 5. **DNA consensus binding analysis for HIF-1α and NF-κB nuclear extracts (1–5 μg) with PDTC.** *A,* HIF-1α activation state at 23→152 and 23→722 torr ΔpO_2 shifts (*FP*, free probe; *NS*, nonspecific), where no stimulatory effects of PDTC are observed. *B,* percentage analysis of the gross cpm relative to the intensity of the band of the control (0) at each pO_2 (**, $p < 0.01$; ***, $p < 0.001$). *C,* NF-κB activation status over ΔpO_2 shifts, where the inhibitory effects are prominent with increasing concentrations of PDTC. *D,* percentage analysis of the gross cpm relative to the intensity of the band obtained without pretreatment (**, $p < 0.01$; ***, $p < 0.001$). The histograms represent the mean values, and the error bars represent the S.E. of the relative intensity of the bands of four independent experiments.

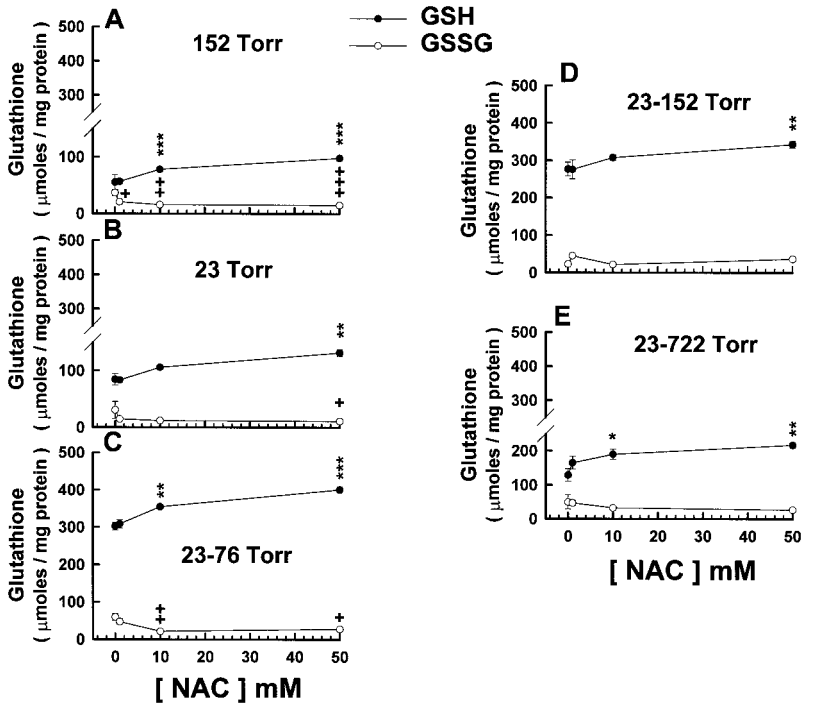

FIG. 6. **Analysis of glutathione homeostasis with NAC pretreatment under various oxygen tensions.** Reduced (●, GSH) and oxidized (○, GSSG) glutathione were enzymatically assessed in fATII cells for the dose-response curves of NAC at (*A*) 152 torr, (*B*) 23 torr, (*C*) 23→76 torr, (*D*) 23→152 torr, and (*E*) 23→722 torr ΔpO_2. Variations are shown such that the elevation of GSH is at the expense of GSSG, thereby increasing GSH/GSSG ratios. *, $p < 0.05$; **, $p < 0.01$; ***, $p < 0.001$ for [GSH], as compared with [GSH] of the control (0 mM NAC). $^{+}$, $p < 0.05$; $^{++}$, $p < 0.01$; $^{+++}$, $p < 0.001$, for [GSSG], as compared with [GSSG] of the control. At all NAC concentrations, [GSH] was significantly higher than [GSSG] ($p < 0.05$). Data are represented as the mean ± S.E.; control (*n = 7), NAC (1 mM, n = 5; 10 mM, n = 5; 50 mM, n = 5). *n refers to number of measurements run in duplicates taken from at least two independent cell preparations, where the entire results were pooled and averaged.

control). PDTC (50 μM) has no stimulatory effects on [GSSG], except at 23→152 (Fig. 7*D*) ΔpO_2 ($^{++}$, $p < 0.001$, as compared with control), whereas it depressed [GSH] at 23→76 and 23→152 torr (Fig. 7, *C* and *D*; **, $p < 0.01$; ***, $p < 0.001$; as compared with control).

Effect of the Ratio of Total to Oxidized Glutathione on HIF-1α and NF-κB Binding Activities in Vitro—The effects of descending ratios (R) of GSH to GSSG were investigated to evaluate HIF-1α and NF-κB activation in nuclear extracts of fATII cells exposed to ascending ΔpO_2 regimen. Increasing GSSG/GSH ratios were shown to be inhibitory on the binding activity of HIF-1α (23 torr, Fig. 8*A*) and NF-κB (23→152 torr, Fig. 8*B*). The most prominent inhibition is obvious with $R \leq 2$ at all oxygen tensions investigated, with complete abrogation at r = 1 (HIF-1α) and r = 1.25 (NF-κB). Linear regression analysis was carried out to determine the inhibitory constants of the negative slopes plotted as percentage of inhibition *versus* the natural logarithm of R. Fig. 8, *C* and *D,* shows the inhibition degrees of HIF-1α and NF-κB activation, respectively. HIF-1α 50% inhibitory constant ($K_i^{\text{HIF-1}\alpha}$) was determined from the negative slope of the equation $y = -13.05x + 89.76$ to be Ln r = 3.05 (r = 21.12); as such, the minimum effective [GSSG] contributing to this inhibition is ~4.73 ± 0.12 μM (Fig. 8*B*). NF-κB 50% inhibitory constant ($K_i^{\text{NF-}\kappa\text{B}}$) was determined from the negative slope of the equation $y = -16.63x + 97.46$ to be Ln r = 2.85 (r = 17.28); as such, the minimum effective [GSSG] con-

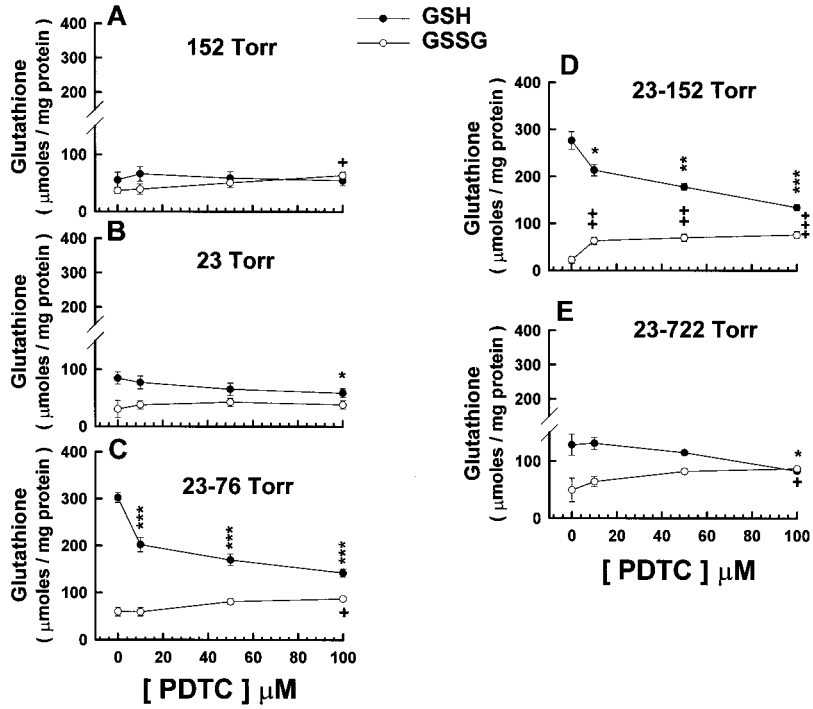

FIG. 7. **Analysis of glutathione homeostasis with PDTC pretreatment under various oxygen tensions.** Reduced (GSH) and oxidized (GSSG) glutathione were enzymatically assessed in fATII cells for the dose-response curves of PDTC at (*A*) 152 torr, (*B*) 23 torr, (*C*) 23→76 torr, (*D*) 23→152 torr, and (*E*) 23→722 torr ΔpO_2. Variations are shown such that the elevation of GSSG is at the expense of GSH, thereby decreasing GSH/GSSG ratios. *, $p < 0.05$; **, $p < 0.01$; ***, $p < 0.001$ for [GSH], as compared with [GSH] of the control (0 μM PDTC)). $^{+}$, $p < 0.05$; $^{++}$, $p < 0.01$; $^{+++}$, $p < 0.001$, for [GSSG], as compared with [GSSG] of the control. Data are represented as the mean ± S.E.; control (*n = 7), PDTC (10 μM, n = 5; 50 μM, n = 5; 100 μM, n = 5). *n refers to number of measurements run in duplicates taken from at least two independent cell preparations, where the entire results were pooled and averaged.

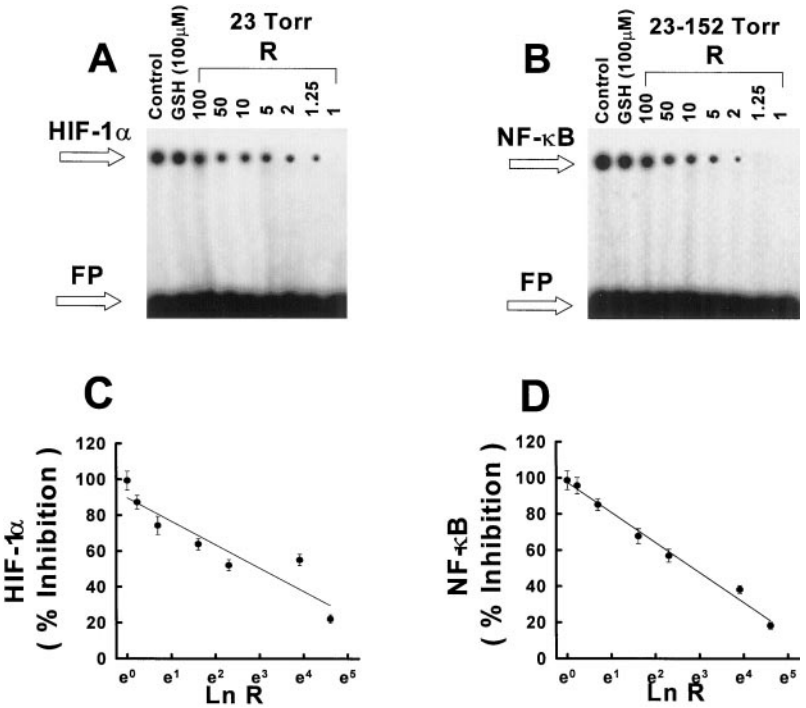

FIG. 8. **Nuclear extracts (5 μg) of fATII cells exposed to oxidative stress were treated *in vitro* with various GSH/GSSG concentrations.** Ratios were adjusted according to the formula ([GSH] + [GSSG])/([GSSG]), such that the molarity of [GSSG] was increased at the expense of [GSH]. *A,* analysis of HIF-1α activation (23 torr) at various ratios (R), with prominent inhibitory effects at $R \leq 1.25$. *B,* analysis of NF-κB activation (23→152 torr) at various R, with maximum inhibitory effects observed at $R \leq 2$. Control lanes contained nuclear extracts without *in vitro* pretreatments, and the lane with 100 μM [GSH] received no exogenous [GSSG] (*FP*, free probe). The dose-dependent decrease in binding activities of either transcription factor is evident with increasing [GSSG]. *C,* linear regression analysis of HIF-1α percentile inhibition (r = 0.93), where the derived inhibitory constant $K_i^{\text{HIF-1}\alpha} \approx 4.73$ μM (see "Results" for more details). *D,* linear regression analysis of NF-κB percentile inhibition (r = 0.99), where the $K_i^{\text{NF-}\kappa\text{B}} \approx 5.78$ μM. This EMSA is representative of results similarly obtained with *in vitro* analysis in three independent experiments of separate cell preparations.

tributing to this inhibition is ~5.78 ± 0.15 μM (Fig. 8*D*).

Cytotoxicity and Cell Viability Assays for Cultures Pretreated with NAC or PDTC—To rule out the possibility that any of the effects mediated by NAC and PDTC are due to cytotoxicity, three independent measures of cell viability were employed. Percentage exclusion of trypan blue in control cell cultures was not significantly different from cultures pretreated with NAC (50 mM) or PDTC (100 μM) ($p > 0.05$, Table IV). The adenylate energy charge ratio did not vary significantly with antioxidant pretreatment, as compared with control cell cultures ($p > 0.05$, Table IV). Finally, measurement of the tetrazolium salt whose ring is cleaved in actively respiring mitochondria of living cells was considered as another assessment of cell viability (Table IV). No significant differences in cell viability are reported with NAC or PDTC pretreatments ($p > 0.05$).

DISCUSSION

The activation of the transcription factors HIF-1α and NF-κB in the distal epithelial lining of the developing lung is redox- and oxygen-sensitive (this study and Ref. 7). To further clarify the molecular mechanisms involved in modulating the genetic response of the fetal lung to oxidative stress, we have focused our attention on the link between cellular antioxidant/pro-oxidant equilibrium and the nuclear translocation and DNA consensus sequence binding (activation) of HIF-1α and NF-κB. To potentiate changes in cellular redox balance through the glutathione biosynthetic pathway, cultures were exposed to an experimental shift in pO_2 with or without NAC,

TABLE IV

Trypan blue exclusion (TBE), energy charge (EC) ratio, and tetrazolium (MTT) reduction as independent measurable indices for cell viability assessment under various ΔpO_2 regimen reported in fATII cells with or without pretreatments with NAC or PDTC for 24 h at 37 °C

Data are mean ± S.E. Control (*n = 4), (NAC, 50 mM; n = 5), and (PDTC, 100 μM; n = 5). $p > 0.05$, as compared to control, without NAC or PDTC pretreatments. *n refers to number of measurements taken from at least three independent cell filters, where the entire results were pooled and averaged.

ΔpO_2	TBE			EC			MTT		
Torr	Control	NAC	PDTC	Control	NAC	PDTC	Control	NAC	PDTC
	%						%		
152	95.62 ± 5.17	92.49 ± 5.45	91.64 ± 7.14	0.77 ± 0.01	0.72 ± 0.04	0.71 ± 0.05	94.82 ± 4.17	93.46 ± 6.49	92.34 ± 7.35
23	93.76 ± 6.25	90.51 ± 4.17	89.37 ± 5.16	0.69 ± 0.01	0.70 ± 0.03	0.69 ± 0.04	95.77 ± 3.82	90.75 ± 7.91	93.56 ± 5.88
23 → 76	96.19 ± 5.87	94.67 ± 5.12	93.09 ± 6.22	0.73 ± 0.02	0.68 ± 0.07	0.70 ± 0.05	94.16 ± 4.55	91.43 ± 6.23	90.05 ± 5.12
23 → 152	92.32 ± 7.84	91.28 ± 5.98	90.56 ± 5.87	0.75 ± 0.01	0.71 ± 0.06	0.68 ± 0.07	93.12 ± 4.62	88.65 ± 6.77	91.79 ± 5.54
23 → 722	94.68 ± 4.18	90.03 ± 7.25	92.45 ± 6.13	0.75 ± 0.03	0.74 ± 0.05	0.72 ± 0.06	96.45 ± 2.23	90.27 ± 8.42	94.86 ± 6.57

a thiol-containing antioxidant and substrate for GSH synthesis (31), or PDTC, possessing both antioxidant thiocarbamate and thiuram pro-oxidant characteristics (22).

NAC induced a significant, dose-dependent increase in HIF-1α nuclear abundance, which was greater under a 23→152 and 23→722 torr ΔpO_2 regimen than observed under stimulating conditions without NAC (23 and 23→76 torr). DNA consensus sequence binding was also preserved at elevated pO_2 at maximal concentrations of NAC employed in this study. These observations suggest that NAC pretreatment effectively manipulate the hypoxia-/redox-dependent signaling sequence, which governs both nuclear abundance and activity of HIF-1α independently from the imposed pO_2 regimen. This is in keeping with the capacity for NAC to suppress and/or scavenge reactive oxygen intermediates (21, 31), thereby imposing a reducing cellular environment, protracting the half-life of cytosolic HIF-1α, and favoring its translocation to the nucleus. As NAC is an acetylated variant of the amino acid L-cysteine, it possesses both direct (*i.e.* oxidizable sulfhydryl groups) and indirect (*i.e.* as a substrate for the biosynthesis of GSH) antioxidant activity (20, 31). To further elucidate the pathways leading to activation of HIF-1α, glutathione concentrations were enzymatically assessed *in vitro* in cultures exposed to 24 h of NAC pretreatment. In this, and a previous study (7), we noted that shifting fATII beyond fetal lung oxygen tensions resulted in an elevated total glutathione pool characterized by a 4-fold rise in [GSH], a modest reduction in [GSSG], and a parallel fall in HIF-1α activity. Although we cannot exclude direct antioxidant buffering by NAC, the observable effect of this compound was to potentiate further both the elevation of [GSH] and reduction of [GSSG] (Fig. 6 and Table I) beyond the shift that occurs naturally with elevated pO_2 regimen. We have previously shown (7) that pretreatment of hypoxic cultures with L-buthionine-(*S,R*)-sulfoximine, an irreversible specific inhibitor of the rate-limiting enzyme in the biosynthesis of glutathione, γ-glutamylcysteine synthetase (γ-GCS) (32), led to a dose-dependent inactivation of HIF-1α, suggesting GSH may be a key modulator of the activity of this factor. In keeping with this, we note that by experimentally increasing GSSG concentrations 4–5-fold in fATII cells using 1,3-*bis*-(2-chloroethyl)-1-nitrosourea or carmustine, an inhibitor of glutathione reductase (GSSG-RD), a partial abrogation of the hypoxia-induced activation of HIF-1α can be achieved, ostensibly by invoking an oxidizing environment.[2] It seems clear, therefore, that the oxygen and ROS responsiveness of HIF-1α resides over a permissive range of antioxidant buffering capacities with the implication that such compounds determine the physiological activity (*i.e.* the *in vivo* K_m) of oxygen-responsive transcription factors to a hypoxia or hyperoxia-linked signal. Fig. 9 presents a schematic summary of the glutathione-linked signaling pathways responsible for the regulation of HIF-1α in fetal distal lung epithelium.

Much recent evidence highlights NF-κB as playing a critical role in coordinating early gene responses to the production of ROS (19), therefore the NAC-induced shift in the glutathione redox state toward a reducing equilibrium would be expected to suppress the activity of this transcription factor. Pretreatment with NAC predictably diminished the hyperoxic nuclear translocation and DNA consensus binding of NF-κB p65 (the major transactivating member of the NF-κB family) in a dose-dependent manner. Indeed, it has been demonstrated that NF-κB activation by a wide variety of stimuli can be blocked by NAC, suggesting that the production of reactive oxygen metabolites is a requisite component of the activation sequence for this transcription factor (33). As ROS generation is rapid, the capacity for NAC to suppress the activation of NF-κB may center largely upon the acute inherent antioxidant characteristics of this compound, although the cellular activity of this transcription factor is favored by a lowered GSH/GSSG incorporating elevated GSSG.

Dithiocarbamates, including PDTC, induce differential effects on redox equilibrium according to: (i) their ability to decrease single electron radical species (a reduction property) and (ii) their capacity to oxidize GSH and related thiol compounds, thereby modulating glutathione recycling potential (an oxidation property; 22, 34). As with other dithiocarbamates, PDTC thus possesses the capacity to exert both anti- and pro-oxidant effects, the former being mediated through dithiocarboxy scavenging of hydrogen peroxide (H_2O_2), superoxide anion ($O_2^{\cdot-}$) (35), and hydroxyl radical (·OH) (36), and the latter being mediated by its oxidation by reactive oxygen and nitrogen species, generating dithiocarbamate thiyl radicals and thiuram disulphides, which directly oxidize GSH to GSSG, a potent regulator of several transcription factors and signal transducing pathways in lung and other systems (36).

In this report we have shown regulated differential effects of PDTC on the activation of HIF-1α and NF-κB, revealing a striking equilibrium between the antioxidant and pro-oxidant modes of action of dithiocarbamates. PDTC, like NAC, induced HIF-1α nuclear translocation at all ΔpO_2 regimen investigated; however, it failed to induce HIF-1α DNA binding activity. We have observed that the GSH/GSSG ratio after PDTC treatment was significantly lowered, largely because of a substantial increase in the rate of GSH oxidation to GSSG (Table II). This decreased ratio may explain why PDTC failed to induce binding to a DNA consensus sequence, as a reducing nuclear environment is mandatory for DNA binding and the expression of hypoxia-responsive genes. This is supported by our observation that HIF-1α consensus DNA binding was facilitated by experimental increases in GSH/GSSG in isolated nuclei (Fig. 8, *A* and *C*). We propose that, although PDTC might be acting as an

[2] J. J. E. Haddad, R. E. Olver, and S. C. Land, unpublished observations.

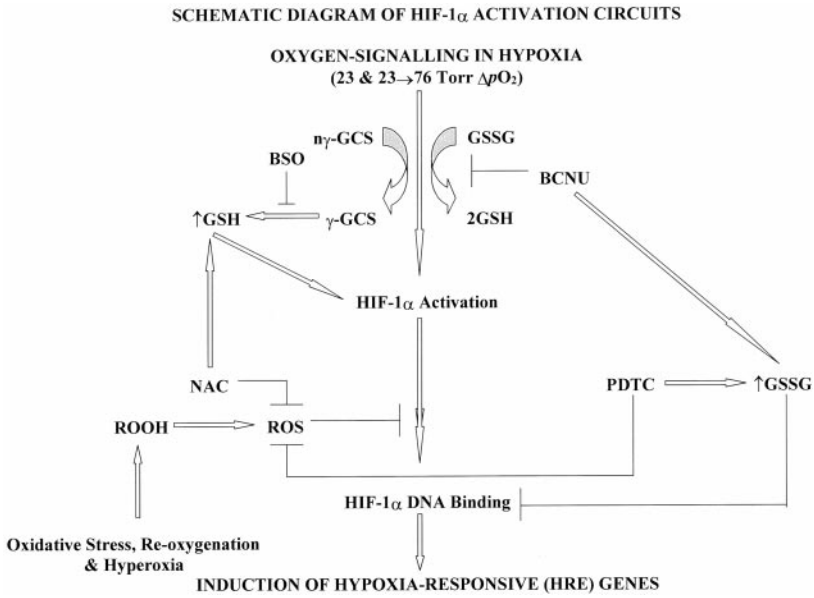

FIG. 9. **Schematic diagram of HIF-1α activation circuits and oxygen-signaling mechanisms in hypoxia.** The reduction of oxidized glutathione (GSSG) forms reduced glutathione (*2GSH*), capable of inducing HIF-1α activation. GSSG recycling to GSH is blocked by 1,3-*bis*-(2-chloroethyl)-1-nitrosourea, a specific glutathione reductase inhibitor, thus increasing intracellular [GSSG], a potent inhibitor of DNA binding. In oxidative stress, γ-glutamylcysteine synthetase is transformed from native, inactive form (*n*γ-*GCS*) to active form (γ-*GCS*), which increases *de novo* synthesis of GSH. This pathway is blocked by L-buthionine-(*S,R*)-sulfoximine, an irreversible inhibitor of γ-GCS, thus affecting HIF-1α activation. ROS, derived from oxygen metabolites (reactive peroxides), tend to block the activation of HIF-1α. NAC, an antioxidant, releases this inhibitory effect by scavenging ROS. NAC, in addition, is a major precursor of GSH, a thiol antioxidant, thereby it elevates [GSH] ($\uparrow$ *GSH*) and induces HIF-1α activation. PDTC is an antioxidant though possessing ROS-scavenging properties, its ability to activate HIF-1α under reducing conditions is not established. PDTC (as a pro-oxidant), like other dithiocarbamates, lowers the GSH/GSSG ratio by oxidizing GSH. The elevated [GSSG] ($\uparrow$ *GSSG*) has the potential to block HIF-1α activation. Upon HIF-1α binding to the hypoxia response element hypoxia-responsive genes are up-regulated.

antioxidant by scavenging ROS, its failure to activate HIF-1α may be attributed to its pro-oxidant properties, whereby the concentration of the oxidized form of glutathione increases favoring a shift in cellular redox toward an oxidizing equilibrium. This is in broad agreement with previous studies showing that PDTC increases the level of GSSG at the expense of GSH (24, 34, 37) and that GSSG affects transcriptional activation by creating oxidizing conditions (24).

PDTC is a potent inhibitor of NF-κB in alveolar epithelia acting at the level of both nuclear translocation as well as consensus sequence binding, being effective at concentrations which are 100–500-fold lower than the inhibitory effect of NAC. This inhibitory effect is likely to be the result of a compound series of events centering around the oxidation of GSH to GSSG (Table II) rather than by any direct interaction with NF-κB itself (PDTC administered at 50 μM to NF-κB-activated fATII-isolated nuclei failed to inhibit DNA consensus sequence binding).[2] Dithiocarbamates are known to inhibit the phosphorylation-dependent release of NF-κB from its cytosolic inhibitory subunit, IκB (38), suggesting that the mechanism of ROS induced activation of this transcription factor involves, at least in part, a redox-responsive kinase activity. However, high GSSG concentrations also promote the formation of a NF-κB-disulfide complex, which inhibits the DNA binding activity of this transcription factor (24). GSSG elevation promotes oxidation of protein cysteinyl thiols, shifting the equilibrium of thiol-disulfide exchange significantly toward the formation of mixed disulfides resulting in a change in protein conformation and subsequent efficiency of DNA binding (12, 39). Notably, we observed that lowered GSH/GSSG in isolated nuclei inhibits NF-κB DNA consensus sequence binding with near identical kinetics to that of HIF-1α (Fig. 8, *B* and *D*). Therefore, although oxidizing cytosolic conditions favor NF-κB dissociation from IκB and subsequent nuclear translocation, a reduced (*i.e.* high GSH/GSSG) nuclear environment favors DNA consensus se-

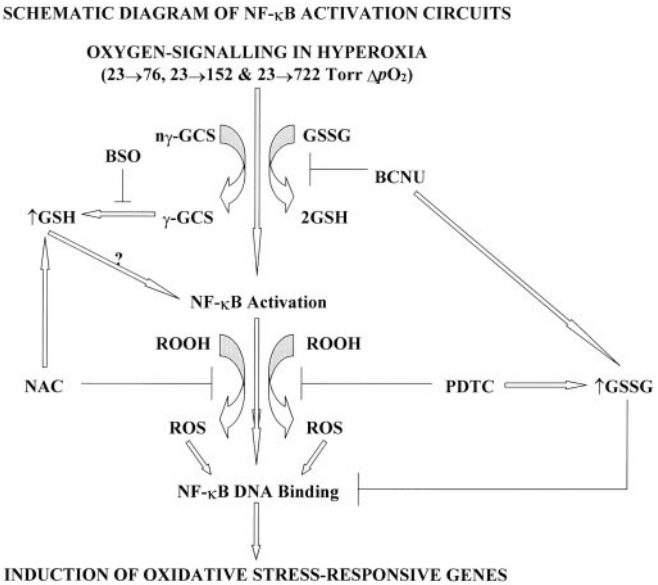

FIG. 10. **Schematic diagram of NF-κB activation circuits and oxygen-signaling mechanisms in hyperoxia.** GSSG reduction to GSH, which is blocked by 1,3-*bis*-(2-chloroethyl)-1-nitrosourea, leads to increasing intracellular stores of [GSSG], a potent inhibitor of NF-κB transcription factor DNA binding. The pathway leading to the formation of GSH by the action of γ-GCS is blocked by L-buthionine-(*S,R*)-sulfoximine, inducing an irreversible inhibition of NF-κB activation. ROS are key components of the pathways leading to the activation of NF-κB, whose binding activity is obliterated by NAC and PDTC, potent scavengers of ROS. Although NAC is elevating [GSH], it is unknown whether this mechanism induces NF-κB activation independently from the antioxidant effects of this inhibitor. PDTC elevates GSSG concentration by GSH oxidation, a pro-oxidant effect characteristic of diothiocarbamates, thereby mediating NF-κB inhibition. Upon NF-κB DNA binding, cascades of hyperoxia-responsive genes are activated, which have the potential to modulate cellular response to oxidative injury.

quence binding. Although we cannot preclude the possibility that PDTC interferes with the translocation of NF-κB to the nucleus, the inhibitory effects of this compound upon NF-κB support the hypothesis that dithiocarbamates primarily act as pro-oxidants by elevating the concentration of oxidized glutathione (GSSG), which is capable of direct (by forming a mixed NF-κB-thiol inactive complexes) or indirect (creating an oxidized environment in the nucleus) abrogation of NF-κB activity. Schematized pathways linking the activation of NF-κB to glutathione equilibrium in the fetal alveolar epithelium are depicted in Fig. 10.

In conclusion, we have demonstrated that NAC and PDTC treatment effectively uncoupled transcription factor activity from the normal pattern induced by changes in oxygen availability in primary cultures of fetal epithelial cells derived from the distal lung. The capacity of the developing lung to mount an adaptive genetic response to hypoxic or hyperoxic environments is therefore determined by the interplay between oxygen availability, reduction-oxidation state cellular compartments (in this case, nuclear and cytosolic) and the glutathione buffering capacity of the alveolar epithelium. The enzymatic component of the glutathione biosynthetic pathway therefore represent a lynchpin for the development of clinical strategies for the treatment of perinatal respiratory syndromes that are linked to oxygen-induced stresses.

REFERENCES

1. Brigham, K. L. (1986) *Chest* **89,** 859–863
2. Chabot, F., Mitchell, J. A., Gutteridge, J. M. C., and Evans, T. W. (1998) *Eur. Respir. J.* **11,** 745–757
3. Müller, J. M., Rupec, R. A., and Baeuerle, P. A. (1997) *Methods: Comp. Methods* **11,** 301–312
4. Dalton, T. P., Shertzer, H. G., and Alvaro, P. (1999) *Annu. Rev. Pharmacol. Toxicol.* **39,** 67–101
5. Griffith, O. W., and Mulcahy, R. T. (1999) *Adv. Enzymol. Relat. Areas Mol. Biol.* **73,** 209–267
6. Meister, A., Griffith, O. W., Novogrodsky, A., and Tate, S. S. (1979) *CIBA Found. Symp.* **72,** 135–161
7. Haddad, J. J. E., and Land, S. C. (2000) *Am. J. Physiol.* **278,** L492–L503
8. Griffith, O. W., Meister, A. (1979) *Proc. Natl. Acad. Sci. U. S. A.* **76,** 5606–5610
9. Rusakow, L. S., Han, J., Hayward, M. A., and Griffith, O. W. (1995) *J. Appl. Physiol.* **79,** 1769–1776
10. Griffith, O. W., and Meister, A. (1978) *J. Biol. Chem.* **253,** 2333–2338
11. Griffith, O. W., and Meister, A. (1985) *Proc. Natl. Acad. Sci. U. S. A.* **82,** 4668–4672
12. Dröge, W., Schulze-Osthoff, K., Mihm, S., Galter, D., Schenk, H., Eck, H. P., Roth, S., and Gmunder, H. (1994) *FASEB J.* **8,** 1131–1138
13. Galter, D., Mihm, S., and Dröge, W. (1994) *Eur. J. Biochem.* **221,** 639–648
14. Menon, S. D., Qin, S., Guy, G. R., and Tan, Y. H. (1993) *J. Biol. Chem.* **268,** 26805–26812
15. Haddad, J. J., and Land, S. C. (1999) *J. Physiol.* (*Lond.*) **517,** 91
16. Huang, L. E., Arney, Z., Livingstone, D. M., and Bunn, H. F. (1996) *J. Biol. Chem.* **271,** 32253–32259
17. Jiang, B.-H., Semenza, G. L., Bauer, C., and Marti, H. H. (1996) *Am. J. Physiol.* **271,** C1172–C1180
18. Gleadle, J. M., and Ratcliffe, P. J. (1998) *Mol. Med. Today* **3,** 122–129
19. Schreck, R., Albermann, K., and Baeuerle, P. A. (1992) *Free Radic. Res. Commun.* **17,** 221–237
20. Bernard, G. R. (1991) *Am. J. Med.* **91,** 55S–59S
21. Moldeus, P., Cotgreave, I. A., and Berggren, M. (1986) *Respiration* **50,** 31–42
22. Orrenius, S., Nobel, C. S., van den Dobbelsteen, D. J., Burkitt, M. J., and Slater, A. F. (1996) *Biochem. Soc. Trans.* **24,** 1032–1038
23. Nobel, C. S., I., Kimland, M., Lind, B., Orrenius, S., and Slater, A. F. G. (1995), *J. Biol. Chem.* **270,** 26202–26208
24. Brennan, P., and O'Neill, L. A. (1996) *Biochem. J.* **320,** 975–981
25. Cotton, R. B. (1998) *Foetal and Neonatal Physiology,* 2nd Ed., pp. 1165–1174 Saunders, PA
26. Wang, G. L., and Semenza, G. L. (1995) *J. Biol. Chem.* **270,** 1230–1237
27. Bergmeyer, H.-U. (1965) *Methods of Enzymatic Analysis,* 2nd Ed., Verlag Chemie, Berlin
28. Bradford, M. M. (1976) *Anal. Biochem.* **72,** 248–254
29. Atkinson, D. E. (1977) *Cellular Energy Metabolism and Its Regulation,* 2nd Ed., Academic Press, New York
30. Denizot, F., and Lang, R. (1986) *J. Immunol. Methods* **89,** 271–277
31. Kelly, G. S. (1998) *Altern. Med. Rev.* **3,** 114–127
32. Griffith, O. W., and Meister, A. (1979) *J. Biol. Chem.* **254,** 7558–7560
33. Schreck, R., Rieber, P., and Baeuerle, P. A. (1991) *EMBO J.* **10,** 2247–2258
34. Schreck, R., Meier, B., Männel, D. N., Dröge, W., and Baeuerle, P. A. (1992) *J. Exp. Med.* **175,** 1181–1194
35. Mankhetkorn, S., Abedinzadeh, Z., and Houee-Levin, C. (1994) *Free Radic. Biol. Med.* **17,** 517–527
36. Liu, J., Shigenaga, M. K., Yan, L. J., Mori, A., and Ames, B. N. (1996) *Free Radic. Res.* **24,** 461–472
37. Wild, A. C., and Mulcahy, T. (1999) *Biochem. J.* **338,** 659–665
38. Traenckner, E. B. M., Pahl, H. L., Schmidt, K. N., Wilk, S., and Baeuerle, P. A. (1995) *EMBO J.* **14,** 2876–2883
39. Toledano, M. B., and Leonard, W. J. (1991) *Proc. Natl. Acad. Sci. U. S. A.* **88,** 4328–4332
40. Meister, A. (1994) *J. Biol. Chem.* **269,** 9397–9400

GENES: STRUCTURE AND REGULATION:

Antioxidant/Pro-oxidant Equilibrium Regulates HIF-1 α and NF-κB Redox Sensitivity: EVIDENCE FOR INHIBITION BY GLUTATHIONE OXIDATION IN ALVEOLAR EPITHELIAL CELLS

John J. E. Haddad, Richard E. Olver and Stephen C. Land

J. Biol. Chem. 2000, 275:21130-21139.
doi: 10.1074/jbc.M000737200 originally published online May 4, 2000